DOI: https://doi.org/10.61841/mej3wp26 Publication URL:https://jarm-s.com/MS/index.php/MS/article/view/50

A NOVEL RICHARDSON EXTRAPOLATION TECHNIQUE ON A SHISHKIN AND EXPONENTIALLY GRADED MESH FOR SINGULARLY PERTURBED CONVECTION-DIFFUSION PROBLEMS WITH INTEGRAL BOUNDARY CONDITIONS

Desta Sodano Sheiso[1]

Department of Mathematics, Indian Institute of Technology Guwahati, Guwahati - 781 039, India[1]

To cite this article:

Sheiso, D. S. . (2024). A NOVEL RICHARDSON EXTRAPOLATION TECHNIQUE FOR NUMERICAL APPROXIMATION OF SINGULARLY PERTURBED CONVECTION-DIFFUSION PROBLEMS WITH INTEGRAL BOUNDARY CONDITIONS. Journal of Advance Research in Mathematics And Statistics (ISSN 2208-2409), 11(1), 25-47. https://doi.org/10.61841/mej3wp26

Corresponding Author:
desta.sodano@iitg.ac.in

ABSTRACT

This study presents the novel Richardson extrapolation techniques for solving numerical approx- imation of singularly perturbed convection-diffusion problems (SPCDP) with integral boundary conditions (IBC). A numerical approach is presented using an upwind finite difference scheme a piecewise-uniform (Shishkin) and exponential (eXp) mesh. To handle the integral boundary con- ditions, the trapezoidal rule is applied. The parameter-uniform error bound for the numerical derivative is established which leading to a first-order convergence rate. The study establishes an error bound for numerical solutions and determines the numerical approximation as well as analyze a upwind finite difference scheme on a piecewise uniform mesh (Shishkin mesh) and exponential (eXp) for singularly perturbed convection diffusion equations with integral boundary conditions. To enhance convergence and accuracy, we utilize Richardson extrapolation. This elevates accuracy from O N −1 ln N to O N −2 ln2 N using this technique, where N is the number of mesh intervals. Numerical results are presented to validate the theoretical findings, demonstrating the effectiveness and accuracy of the proposed technique.
Subject Classification: AMS 65L11, 65L12, 65L20, 65L70, 65R20 AMS 65M06, 65M12, 65M15.

KEYWORDS*:* *Singularly Perturbed Problems, Richardson extrapolation, Upwind finite difference scheme scheme, IBC, Piecewise-uniform mesh, exponential graded (eXp) mesh.*

AMS Subject Classification: AMS 65L11, 65L12, 65L20, 65L70, 65R20 AMS 65M06, 65M12, 65M15.

Introduction

This article investigates the convection-diffusion type's singularly perturbed differential equations (SPDE) with integral boundary conditions (IBC). Integral boundary conditions are indeed neces- sary and commonly employed when studying SPCDP [35, 34, 1, 2, 4, 21]. Such boundary value problems (BVP) with IBC are commonly encountered in various domains, including electrochem- istry, thermoelasticity, heat conduction, etc. Only a few authors [1, 10, 18] have addressed SPDE with integral boundary conditions. Singular perturbation problems (SPPs) arising in the context of convection-diffusion problems with integral boundary conditions are prevalent across various fields of applied mathematics and engineering [3, 33]. BVPs with integral boundary conditions multiply- ing the leading derivative term by a small parameter ε are called singularly perturbed problems with integral boundary conditions.

SPCDP exhibits a characteristic where a small parameter $\varepsilon(0 < \varepsilon \ll 1)$ multiplies some or all of the highest-order terms in the differential equation. This parameter represents the degree of perturbation in the system and significantly influences the solution's behavior. The Navier-Stokes equation, governing fluid flow dynamics, is an example of a SPCDP [32]. Introducing the small parameter ε, the equation becomes:

$$\varepsilon^2\left(\frac{\partial^2 u}{\partial x^2}+\frac{\partial^2 u}{\partial y^2}\right)+\frac{\partial(u^2+\hat{p})}{\partial x}+\frac{\partial(uv)}{\partial y}=\left(\frac{1}{Re}\right) \tag{1.1}$$

where u and v represent velocity components along x and y directions, respectively, and p^ denotes pressure. The Reynolds number Re is a dimensionless parameter relating to the fluid's length scale, velocity scale, and kinematic viscosity. At large Reynolds numbers (Re), the equation transforms into a SPCDP with intergal boundary conditions. The diffusion terms $\frac{\partial^2 u}{\partial x^2}$ and $\frac{\partial^2 u}{\partial y^2}$ are scaled by ε2, indicating their relatively smaller influence compared to the convective terms $\frac{\partial(u^2+\hat{p})}{\partial y}$ and $\frac{\partial(uv)}{\partial y}$.

The small parameter ε signifies the existence of a boundary layer where the solution exhibits rapid variations. SPCDPs involve significant contributions from both convection and diffusion, with ε amplifying either the convection or diffusion term in the equations. Finite Difference Methods (FDMs) are commonly used to approximate such solutions, though research on approximating their derivatives has been relatively limited. These approximations are valuable in certain applications like flux or flag calculations. SPPs, characterized by a small parameter $\varepsilon(0 < \varepsilon \ll 1)$ multiplying the highest derivative term, have been extensively studied in the field of differential equations [15, 30]. These problems exhibit rapid changes in the solution within specific domain regions. To obtain accurate numerical solutions for such problems, it is essential to develop appropriate approaches that provide error estimates independent of the small parameter. One of the most straightforward and practical approaches for developing such methods involves employing a category of piecewise uniform (Shishkin) mesh. Numerical methods for equations with non-local boundary conditions have also been widely investigated [2].

The Shishkin mesh and exponentially graded mesh are two effective techniques for solving SPCDPs [2, 21, 34]. The Shishkin mesh is a piecewise-uniform mesh that incorporates two uniform segments, transitioning at a point determined by the singular perturbation parameter. This design allows for a refined mesh in regions where the solution exhibits sharp gradients or boundary layers, effectively balancing discretization errors across the entire domain. On the other hand, the expo- nentially graded mesh employs a geometric progression of mesh points, concentrating more points in areas where the solution varies rapidly, such as boundary layers[12]. This approach enables a more accurate representation of the solution in critical regions by decreasing mesh size exponen- tially towards these areas. By combining Richardson extrapolation with these two mesh types, the proposed technique aims to enhance the accuracy of numerical approximations for SPCDPs with integral boundary conditions. This innovative approach leverages the strengths of Richardson extrapolation and the adaptability of both mesh types, potentially yielding highly precise solutions even in the presence of challenging features such as boundary layers and singular perturbations [4]. Richardson extrapolation has been employed by various scholars as a technique to solve SPCDPs with non-local boundary conditions. Relevant works include what is mentioned in the reference (for example [11, 14, 20, 23, 36]). The primary goal of this work is to present Richardson's extrapolation to improve numerical solution accuracy and efficiency, as well as to investigate and analyze and post-processing method. This improvement in convergence rate is particularly targeted for prob- lems that are discretized using a Shishkin mesh [25]. The development of SPCDPs with non-local boundary conditions arises from the need to accurately model physical phenomena exhibiting both convective and diffusive behavior while considering non-local effects at the boundaries. Studying

SPCDPs with non-local boundary conditions aims to accurately represent specific systems' behavior, enhancing the methods' accuracy, stability, and efficiency. The use of these techniques improves the effectiveness of investigating real-world events and allows for consistent results in a wide range of applications [7].

M. Cakir and G. M. Amiraliyev [4, 5] developed a second-order numerical method for SPPs with non-local boundary conditions, and investigated FDM for the same problem with non-local boundary conditions. Amiraliyev and Raja [1], focus on the well-posedness of SPDEs with non-local boundary conditions. These works will investigate solutions' existence, uniqueness, and stability to ensure that the issue is well-posed. On the other hand, Kopteva and Stynes [17, 25, 36] focus on obtaining derivative approximations in SPCDPs that consider scale variations between the boundary layer region and the outer region. Their research addresses SPCDPs where the convection and diffusion terms exhibit significantly different magnitudes. They aim to accurately capture the solution behavior in different problem regions by appropriately scaling the derivatives. As the $\varepsilon(0 < \varepsilon \ll 1)$ approaches zero, the derivative solution of SPDE becomes unbounded. To approximate these derivatives accurately, scaling techniques are necessary.

R. Mythili Priyadharshini and N. Ramanujam have focused on developing approximation tech- niques for computing scaled first and second derivatives, as detailed in their works [24, 27]. Recently, Desta Sodano [33] advanced this field by developing Richardson extrapolation for SPCDPs with non-local boundary conditions using scaled derivatives.

One of the main objectives of their research is to address the numerical approximation of deriva- tives, especially in the context of problems with disparate scales or SPPs. They propose and develop innovative techniques for approximating derivatives. The research conducted by Desta Sodano [33] as well as Debela et al[12] presents a significant advancement in the field of numerical methods for solving SPCDPs with integral boundary conditions. Later, Debela and Duressa proposed a com- putational method for the class of SPCDE with IBC using the Richardson extrapolation technique in [10]. The main contribution of Debela and Duressa's research is the development of a stable numerical method to effectively tackle SPCDPs with integral boundary conditions (IBC).

This paper represents the inaugural analysis of Richardson extrapolation on the exponentially graded mesh applied to singularly perturbed parabolic convection-diffusion IBVPs through error decomposition after extrapolation.Initially, we address the SPCDP (2.1) on both a Shishkin mesh and an exponentially graded mesh using the classical implicit upwind finite difference scheme. We then demonstrate that this implicit upwind scheme achieves ε-uniform convergence with nearly first-order accuracy in the discrete supremum norm. Following this, we apply the Richardson extrapolation technique to enhance the nearly first-order convergence of the simple upwinding method, achieving an almost second-order convergence.

Motivated by these considerations, we proposed using the Richardson extrapolation technique to solve SPCDPs with integral boundary conditions (2.1). To the best of our knowledge, the authors' approach began with proposing an approximation method for scaled solution derivatives. We worked on problems with upwind schemes on a Shishkin mesh and exponentially graded mesh, obtaining approximately a first-order convergence rate. The authors most likely used Richardson extrapolation on the upwind finite difference method (FDM) within the Shishkin mesh as well as exponentially graded mesh to improve accuracy from almost first to almost second order.

The rest of the article is organized as follows: Section 2, defines problems with non-local boundary conditions and presents analytical results. Section 3, introduces a numerical method based on an upwind FDM. Section 4, includes numerical examples to validate the theoretical results. In Section 5, the paper provides final conclusions. Throughout the paper, C refers to a generic constant independent of ε and discretization parameters N.

PROBLEMS WITH INTEGRAL BOUNDARY CONDITIONS (IBC) AND SOME ANALYTICAL RESULTS

$$\begin{cases} \mathcal{L}\xi(x) = -\varepsilon\xi''(x) + \mu(x)\xi'(x) + \eta(x)\xi(x) = f(x), \quad x \in \Omega, \\ \xi(0) = \xi_0, \quad \xi(1) - \varepsilon \int_0^1 g(x)\xi(x)dx = l_2 \end{cases} \tag{2.1}$$

where $0 < \varepsilon \ll 1$ is a singular perturbation parameter and the coefficient functions $\mu(x)$, $\eta(x)$ are smooth, bounded and satisfy $\mu(x) \geq \alpha > 0$, $\eta(x) \geq \beta > 0$, $x \in \bar{\Omega}$. The function $g(x)$ is non-negative, and it satisfies 1 $g(x)dx < 1$. The above problem satisfies the maximum principle and stability result. The detail proof is given in [1, 4, 29].

Analytical results

To develop sharp bounds we write the analytical solution in the form $\xi(x) = p(x) + q(x)$, where $p(x)$ is the smooth component and $q(x)$ is the singular component. The smooth component $p(x)$ can be expressed as an asymptotic expansion $p(x) = p_0(x) + \varepsilon p_1(x) + \varepsilon^2 p_2(x)$ satisfies the following equations

$$\mu(x)p_0'(x) + \eta(x)p_0(x) = f(x), \quad p_0(0) = \xi(0), \tag{2.2}$$

$$\mu(x)p_1'(x) + \eta(x)p_1(x) = p_0''(x), \quad p_1(0) = 0, \tag{2.3}$$

$$-\varepsilon p_2''(x) + \mu(x)p_2'(x) + \eta(x)p_2(x) = p_1''(x), \quad p_2(0) = 0. \tag{2.4}$$

Hence, the smooth component of the solution satisfies

$$\begin{cases} \mathcal{L}_0 p_0 = f(x), \quad p_0(0) = \xi_0, \\ \mathcal{L}_0 p_1 = p_0'', \quad p_1(0) = 0. \end{cases} \tag{2.5}$$

Now, we must extend the scaling to the point where $x = 1$. Consequently, the differential operator $\mathcal{L} = \varepsilon\mathcal{L}_1 + \mathcal{L}_0$ gets converted to $\mathcal{L} = \varepsilon\mathcal{L}_1^* + \mathcal{L}_0^*$, where reduced differential operator $\mathcal{L}_0^* = -\dfrac{d^2}{dz^2} - \mu_0\dfrac{d}{dz}$ and $\mathcal{L}_1^* = -\mu_1 Z\dfrac{d}{dz} + \eta_0$.

Therefore, the boundary component of the solution satisfies the following conditions:

$$\begin{cases} \mathcal{L}_0^* q_0 = 0, \\ \mathcal{L}_0^* q_i = -\sum_{j=1}^{i} \mathcal{L}_j^* q_{i-j}, \quad \text{for} \quad i = 1, \ldots, m+1, \\ q_j(0) = -p_j(1) + l_2 + \int_0^1 g(x)\xi(x)dx, \quad \text{for} \quad j = 0, \ldots, 3, \\ \lim_{z\to\infty} q_i(z) = 0, \end{cases} \tag{2.6}$$

we choose $q(z) = \sum_{i=0}^{m+1} \varepsilon^i q_i(z)$.

Theorem 2.1. Let $\xi(x)$ be the solution of (2.1) and $p0(x)$ be the solution of (2.5). Then, there exists a constant $C > 0$ such that for all $x \in \bar{\Omega}$, we have

$$|\xi(x) - p0(x)| \le C\, 1 + e^{-\alpha(1-x)/\varepsilon}. \qquad (2.7)$$

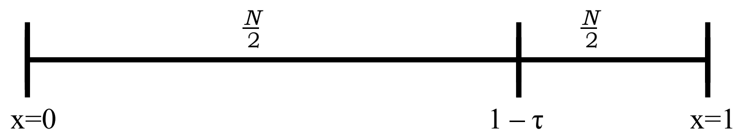

Figure 1: The Piecewise Uniform Mesh ΩN

Proof. The detailed proof is given in [22].

Lemma 2.2. The solution ξ can be decomposed into the sum $\xi = p + q$, where $p(x)$ is the smooth component and $q(x)$ is the boundary component respectively. Furthermore, these components and their derivatives satisfy the following bounds:

$$\|p^{(k)}(x)\|_{\bar{\Omega}} \le C\left(1 + \varepsilon^{(2-k)}\right), \qquad 0 \le k \le 4, \qquad (2.8)$$

$$\|q^{(k)}(x)\| \le C\varepsilon^{-k} e^{-\alpha(1-x)/\varepsilon}, \quad 0 \le k \le 4, \qquad \forall x \in \bar{\Omega}. \qquad (2.9)$$

Proof. The detail proof is given in [4, 13]. The detailed proof of the lemma can be established by utilizing appropriate barrier functions, making use of Theorem 1, and employing the proof technique described in the reference [13] (p. 46).

NUMERICAL METHODS

This section discusses the mesh selection strategy for solving the problem (2.1). We concentrate on the piecewise uniform mesh. The numerical computations use an upwind FDM, which accounts for non-local boundary conditions.

Mesh Generation

Construction of piecewise-uniform (Shishkin) mesh

This mesh is extensively discussed in the references [8, 14, 19, 25]. To effectively handle the boundary layer at $x = 1$ in the SPCDPs with non-local boundary conditions (2.1), we utilize a piecewise-uniform mesh. This mesh includes a transition point at $1 - \tau$, where

$$\tau = \min\left\{\frac{1}{2}, \frac{2\varepsilon}{\alpha} \ln N\right\}.$$

To ensure numerical solvability, we choose the parameter τ based on a specific condition:

$$\tau = \frac{2\varepsilon}{\alpha} \ln N, \qquad (3.1)$$

where N is significantly larger than $\frac{1}{\varepsilon}$.

A piecewise-uniform mesh is constructed by dividing the domain $\Omega = [0, 1]$ into two sub-intervals: $[0, 1 - \tau]$ and $[1 - \tau, 1]$. Each sub-interval is uniformly subdivided into N/2 intervals to create the mesh. To represent the mesh points in the interior and boundary regions of the Shishkin mesh, we define two sets: $\Omega_1^N = \{x_i\}_{i=0}^N$, where $x_0 = 0$ and $x_N = 1$. The mesh widths $h_i = x_i - x_{i-1}$. satisfy

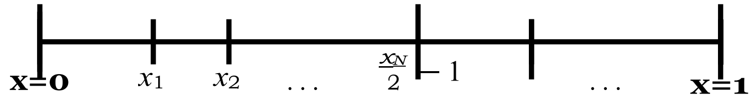

Figure 2: The exponentially graded (exp) mesh distribution

$h_i = H$ for $i = 1, \ldots, N/2$ and $h_i = h$ for $i = N/2 + 1, \ldots, N$. Now, according to the definition of x_i's, the spatial mesh sizes can be expressed as follows:

$$h_i = \begin{cases} H = \dfrac{2(1-\tau)}{N}, & \text{for} \quad i = 1, \cdots, \dfrac{N}{2}, \\ h = \dfrac{2\tau}{N}, & \text{for} \quad i = \left(\dfrac{N}{2}\right) + 1, \cdots, N. \end{cases} \tag{3.2}$$

H and h represent the spatial mesh sizes in [0, 1 − τ] and [1 − τ, 1], respectively. The piecewise- uniform mesh, denoted as ΩN , is entirely defined by user-specified parameters N and τ . The interior mesh points are given by:

$$\Omega_1^N = \{x_i : 1 \le i \le N/2\} \bigcup \{x_i : N/2 + 1 \le i \le N\}. \tag{3.3}$$

It is clear that $\bar{\Omega}_1^N =\cdot \{x_i\}_{i=0}^N$. The step between consecutive interior mesh points is given by

$\hat{h} = h_{i+1} + h_i$. while the step for boundary mesh points is $\hbar = \frac{h_{i+1}+h_i}{2}$. Interior mesh points step: $\hat{h} = h_{i+1} + h_i$; Boundary mesh points step: $\hbar = \frac{hi+1+hi}{2}$.

Construction of Exponentially Graded (eXp) mesh

The eXp mesh, designed with an exponential grading strategy, will be specifically constructed to approximate the characteristics of the typical boundary layer function. To discretize the interval I = (0, 1) using the eXp mesh, we initialize the process by selecting an even number N > 2. The interval [0, 1] is divided into N sub-intervals in order to construct an eXp mesh, denoted as Ii, using nodal points {xi}N . The size of each subinterval, hi = |xi − xi−1|, is determined by the difference between consecutive nodal points, where i = 1, . . . , N .

We denote the space of polynomials with degree ≤ p as Pp(I). Next, we partition the domain $\bar{\Omega}$ into two subdomains, namely $\bar{\Omega} = \Omega_1 \cup \Omega_2$, where

$$\Omega_1 = [0, x_{N/2-1}] \quad \text{and} \quad \Omega_2 = [x_{N/2-1}, 1].$$

In addition, we partition the subinterval Ω_2 into N/2 + 1 equidistant mesh points, while the subin- terval Ω_1 is divided into N/2 − 1 mesh points using the eXp mesh. To generate this mesh, we introduce a mesh-generating function ϕ that fulfills the condition ϕ(0) = 0. The specific form of the mesh generating function can be found in Constantinou [9] and Xenophontos [37] , as well as in the work of Podila et al. [26], where more detailed information is available. It is important to mention that we do not explicitly identify a transition point; rather, we generate the eXp mesh on the interval (0, 1) and consider xN/2−1 as our transition point for the transition. In order to discretize the interval I = (0, 1) using an exponentially graded mesh, we follow the steps outlined below: Step 1: Define the mesh-generating function ϕ(t) as:

$$\phi(t) = -\ln\left[1 - 2\chi_{p,\varepsilon} t\right], \quad t \in \left[0, \frac{1}{2} - \frac{1}{N}\right]$$

where $\chi_{p,\varepsilon} = 1 - \exp\left(-\frac{\beta}{(p+1)\varepsilon}\right)$. Step 2: Compute the nodal points x_i in the subinterval $[0, N/2-1]$ using the formula:

$$x_i^* = \frac{\varepsilon}{\beta}(p+1)\phi\left(\frac{i}{N}\right), \quad i = 0, \ldots, \frac{N}{2} - 1.$$

Here, ε is a small value for numerical stability, β is a constant, p is the degree of polynomials in the space $\mathcal{P}_p(I)$, and $i = 0, ..., N/2-1$.
Step 3: Compute the mesh points x_i on the interval I of an exponential-type mesh are as follows:

$$x_k = \begin{cases} 2k\dfrac{\frac{x_N^*}{2} - 1}{1+N}, & k = 0, \ldots, \frac{N}{2} + 1, \\ 1 - x_{N-1}^*, & k = \frac{N}{2} + 1, \ldots, N. \end{cases} \tag{3.4}$$

3.2. Numerical Scheme

The discrete problem corresponding to (2.1) is as follows: Find $Z^N(x_i)$ such that

$$\begin{cases} \mathcal{L}^N Z^N(x_i) = -\varepsilon\delta^2 Z^N(x_i) + \mu(x_i)D^- Z^N(x_i) + \eta(x_i)Z^N(x_i) = f(x_i), & \forall x_i \in \bar{\Omega}^N, \\ Z^N(0) = \xi_0, \quad Z^N(x_N) - \varepsilon\sum_{i=1}^N \frac{g(x_{i-1})Z^N(x_{i-1}) + g(x_i)Z^N(x_i)}{2}h_i = l_2. \end{cases} \tag{3.5}$$

where the first and second-order finite differences are defined as

$$D^- Z^N(x_i) = \frac{Z^N(x_i) - Z^N(x_{i-1})}{h_{i-1}},$$

$$\delta^2 Z^N(x_i) = \frac{-2\varepsilon}{h_i + h_{i+1}}\left(\frac{Z^N(x_{i+1}) - Z^N(x_i)}{h_{i+1}} - \frac{Z^N(x_i) - Z^N(x_{i-1})}{h_i}\right).$$

Note: The above numerical scheme satisfies the discrete maximum principle and discrete stability result. Hence, the matrix associated with this scheme is an M-Matrix.
Equation (3.5) can be expressed as the following system of algebraic equations:

$$\begin{cases} -r_i^- Z_{i-1}^N + r_i^c Z_i^N + r_i^+ Z_{i+1}^N = f_i, \quad i = 1, \ldots, N-1, \\ Z^N(0) = \xi_0, \quad Z^N(x_N) - \varepsilon\sum_{i=1}^N \frac{g(x_{i-1})Z^N(x_{i-1}) + g(x_i)Z^N(x_i)}{2}h_i = l_2. \end{cases} \tag{3.6}$$

where the coefficients in the upwind finite difference scheme are given by

$$\begin{cases} r_i^- = \left(\frac{-2\varepsilon}{h_{i+1}(h_i + h_{i+1})} - \frac{\mu_i}{h_{i-1}}\right), \\ r_i^c = \left(\frac{2\varepsilon}{h_{i+1}(h_i + h_{i+1})} + \frac{2\varepsilon}{h_i(h_i + h_{i+1})} + \frac{\mu_i}{h_{i-1}} + \eta_i\right), \\ r_i^+ = \left(\frac{2\varepsilon}{h_{i+1}(h_i + h_{i+1})}\right). \end{cases} \tag{3.7}$$

Theorem 3.1. *Let ξ be the solution of (2.1) and Z^N be the numerical solution defined by (3.5). Then, the following inequality holds:*

$$\left|\xi(x_i) - Z^N(x_i)\right| \le CN^{-1}\ln N, \quad \forall x_i \in \bar{\Omega}^N.$$

`where C is a constant independent of ε and N.
Proof. The detailed proof can be found in [28].
Prior to the extra polation analysis, we introduce a crucial lemma for the subsequent section. We define the piecewise (0,1)-Pade approximation of exp −αxi ε on the meshΩN 1 ,wherei=0,1,...,N, as the following mesh functions.

$$S_i = \prod_{k=1}^{i}\left(1+\frac{\alpha h_k}{\varepsilon}\right), \quad S_i' = \prod_{k=1}^{i}\left(1+\frac{\alpha h_k}{2\varepsilon}\right)$$

then $S_i \geq \exp(\frac{-\alpha x_i}{\varepsilon})$,where by convection $S_0 = S_0' = 1$.
The numerical scheme for an upwind scheme (3.5) on Ω^N can be expressed as follows: For $i = 1,\ldots,N-1$,

$$\mathcal{L}^N Z^N(x_i) = \frac{-2\varepsilon}{h_i+h_{i+1}}\left(\frac{Z_{i+1}-Z_i}{h_{i+1}} - \frac{Z_i - Z_{i-1}}{h_i}\right) + a_i\left(\frac{Z_i - Z_{i-1}}{h_i}\right) + b_i Z_i$$

$$\mathcal{L}^N S(x_i) = \frac{-2\varepsilon}{h_i+h_{i+1}}\left(\frac{\left[S_i(1+\frac{\alpha h_{i+1}}{\varepsilon})\right] - S_i}{h_{i+1}} - S_i - \frac{S_i}{(1+\frac{\alpha h_{i-1}}{\varepsilon})}\right) + \mu_i\left(S_i - \frac{S_i}{(1+\frac{\alpha h_{i-1}}{\varepsilon})}\right) + \eta_i S_i,$$

$$S(x_N) - \varepsilon\sum_{i=1}^{N}\frac{g(x_{i-1})S(x_{i-1}) + g(x_i)S(x_i)}{2}h_i = l_2.$$

Lemma 3.2. *The mesh functions S_i satisfy the following property for $i = 1,\ldots,N-1$: there exists a positive constant C such that*

$$\mathcal{L}^N S_i \geq \frac{C}{\varepsilon+\alpha h_i}S_i \quad \textit{and} \quad \mathcal{L}^N S_i' \geq \frac{C}{2\varepsilon+\alpha h_i}S_i'. \tag{3.8}$$

Furthermore, for $i = N/2+1,\ldots,N-1$, there exists a constant C_1 such that

$$\mathcal{L}^N S_i \geq \frac{C_1}{\varepsilon}S_i \quad \text{and} \quad \mathcal{L}^N S_i' \geq \frac{C_1}{\varepsilon}S_i'. \tag{3.9}$$

Proof. The detailed proof can be found in [25]

Richardson extrapolation Technique
This article aims to enhance the accuracy of the upwind scheme (3.5) using Richardson extrapolation, which has proven to improve numerical solutions for differential equations [31].
The ξ^N (x) is computed on the mesh ΩN and Ω2N . This mesh has 2N sub-intervals and the transition point $1-\tau$ as Ω_1^N. The two meshes are interconnected, that is, $\Omega_1^N = \{x_i\} \subset \Omega_1^{2N} = \{\hat{x}_i\}$. Thus, on Ω_1^{2N}, the following conditions hold: $\hat{x}_i - \hat{x}_{i-1} = H/2$ for $\hat{x}_i \in [0, 1-\tau)$ and $\hat{x}_i - \hat{x}_{i-1} = h/2$ for $\hat{x}_i \in (1-\tau, 1]$.
Clearly Ω_1^{2N} be the mesh obtained by bisecting the mesh intervals in Ω_1^N, and let ξ^N represent the approximation of the solution on Ω_1^{2N}. Thus, Ω_1^N is a subset of Ω_1^{2N}, and similarly, Ω_2^N is a subset of Ω_2^{2N}. We proved that

$$\left(\xi(x_i) - Z^N(x_i)\right) = CN^{-1}\ln N + R_N(x_i), \quad x_i \in \Omega_1^N, \tag{3.10}$$

where C is a constant independent of mesh size h_i and ε. The remainder term $R_N(x_i) \le Ch_i^2$.

$$R_N(x_i) \le C \max_{i=1,\dots,N} \left| \frac{1}{2} \sum_{i=1}^{N} \int_{x_{i-1}}^{x_i} (x_i - \zeta)(x_{i-1} - \zeta) f''(\zeta) d\zeta \right| \le Ch_i^2, \quad \zeta \in [x_{i-1}, x_i].$$

Given that equation (3.10) holds for all $h \neq 0$, we can deduce the following relation for $x_i \in \Omega_1^N$:

$$\left(\xi(x_i) - Z^N(x_i)\right) = CN^{-1}(\ln N)^2 + R_N(x_i), \tag{3.11}$$

where $R_N(x_i)$ represents the remainder error term, and $R_N(x_i) = \mathcal{O}(h^2)$.
Now, from the definition of transition parameters $\tau = \dfrac{2\varepsilon}{\alpha} \ln N$ and $\ln N = \dfrac{\alpha\tau}{2\varepsilon}$. Substituting $\ln N$ into (3.10), we find that $\bar{\Omega}_1^{2N}$ is solved using the same $1 - \tau$ transition point:

$$\xi(x_i) - Z^{2N}(x_i) = C(2N)^{-1} \left(\frac{\alpha\tau}{2\varepsilon}\right) + R_{2N}(\hat{x}_i), \quad \text{for all} \quad \hat{x}_i \in \Omega_1^{2N}, \tag{3.12}$$

where Z^{2N} denotes the solution of discrete problem (3.5) and where the remainders $R_{2N}(x_i)$ are $o(N^{-1}\ln^2 N)$. Then multiply equation (3.12) by 2, then we get

$$2\xi(x_i) - 2Z^{2N}(x_i) = \frac{C}{N} \left(\frac{\alpha\tau}{2\varepsilon}\right) + 2R_{2N}(x_i), \quad x_i \in \Omega_1^N. \tag{3.13}$$

Subtracting equation (3.13) from equation (3.10) or eliminating the initial term $O(N^{-1})$ from both equations, we acquire:

$$\xi(x_i) - \left(2Z^{2N}(x_i) - Z^N(x_i)\right) = R_N(x_i) - 2R_{2N}(x_i), \quad x_i \in \Omega_1^N \tag{3.14}$$

which is equal to $o(N^{-1}\ln^2 N)$.
The truncation error of the remainder R_N originates from combining the first-order derivative difference scheme and the trapezoidal rule's truncation error for a non-uniform mesh. Thus, the approximation for the truncation error of the remainder R_N from equation (3.14) is as follows:

$$Z - \xi \approx N^{-1}\ln N + O(N^{-2}).$$

This suggests that the Richardson extrapolation technique enhances the convergence rate from almost first-order to almost second-order.

3.3.1. Discrete solution decomposition

Analogous to the continuous solution, we can decompose the discrete solution Z^N into the following sum $Z^N(x_i) = P^N(x_i) + Q^N(x_i)$, where P^N represents the smooth component and satisfies the following discrete problems:

$$\begin{cases} \mathcal{L}^N P^N(x_i) = f(x_i), & x_i \in \Omega_1^N \\ P^N(0) = p(0), & P^N(x_N) = p(1), \end{cases} \tag{3.15}$$

and Q^N represents the boundary component, and satisfies the following discrete problem:

$$\begin{cases} \mathcal{L}^N Q^N(x_i) = 0, & x_i \in \Omega_1^N \\ Q^N(0) = q(0), & Q^N(x_N) = q(1). \end{cases} \tag{3.16}$$

Now, we can express the error as follows: $\left(Z^N - \xi\right)(x_i) = \left(P^N - p\right)(x_i) + \left(Q^N - q\right)(x_i)$. Following a similar approach, we define $Z^{2N}(x_i) = P^{2N}(x_i) + Q^{2N}(x_i)$ to continue the decomposition. Thus, the error in the discrete solution is presented by decomposing the solution Z^N over Ω_1^N as described in equations (3.15) and (3.16):

$$\left(Z^N - \xi\right)(x_i) = \left(P^N - p\right)(x_i) + \left(Q^N - q\right)(x_i)$$

and

$$\left(Z^{2N} - \xi\right)(x_i) = \left(P^{2N} - p\right)(x_i) + \left(Q^{2N} - q\right)(x_i).$$

3.3.2. Extrapolated solution of P^N

Let's first consider the error in the smooth part of ξ, denoted by $P^N(x_i) - p(x_i)$. The lemma provides the bound for the truncation error p.

Lemma 3.3. *Assuming $\varepsilon \leq N^{-1}$ and for all $x_i \in \Omega$, we can calculate the local truncation error for the smooth component p in the following way:*

$$\mathcal{L}^N(P^N - p)(x_i) = O(H^2) + \frac{1}{2}\mu(x_i)(x_{i+1} - x_i)p''(x).$$

Proof. Based on the bounds established in [22], where $\left|p^{(k)}(x)\right| \leq C(1+\varepsilon^{2-k})$ for $0 \leq k \leq 4$ and all $x \in [0,1]$, we can use Lemma 2.2 for derivative bounds on p, along with Taylor's series expansion, to derive the following equation:

$$\mathcal{L}^N(P^N - p)(x_i) = \frac{\varepsilon}{3\hat{h}_i}\left[h_{i+1}^2\frac{\partial^3 p}{\partial x^3}(\chi_1) - h_i^2\frac{\partial^3 p}{\partial x^3}(\chi_2)\right] + \frac{h_i}{2}\mu(x_i)\frac{\partial^2 p}{\partial x^2}(x_i) - \frac{h_i^2}{3!}\mu(x_i)\frac{\partial^3 p}{\partial x^3}(\chi_1) - h_i^2\frac{\partial^3 p}{\partial x^3}(\chi_2),$$

where $\chi_1 \in (x_i, x_{i+1})$ and $\chi_2 \in (x_{i-1}, x_i)$.
For every x in Ω, $\tilde{E}$ is defined as a non-local solution to the boundary value problem using Keller's classical approach [16].
The function $\tilde{E}$ is defined as the solution to the following BVP:

$$\mathcal{L}\tilde{E}(x) = \Phi(x), \quad \tilde{E}(0) = \tilde{E}(1) = 0, \quad \forall x \in \Omega. \tag{3.17}$$

where $\Phi(x)$ is given by $\Phi(x) = \dfrac{1}{2}\mu(x_i)(x_{i+1} - x_i)p''(x)$.
Now, let $\mu \in C^2[0,1]$ and $p \in C^4[0,1]$ with their derivatives bounded as in (2.8). As a result, $\Phi \in C^2[0,1]$ satisfies $|\Phi| \leq C$ and $\Phi'(x) \leq C$. Therefore, $\tilde{E}$ can be decomposed into $\tilde{E} = \psi + \lambda$, where ψ and λ represent the smooth and boundary parts of $\tilde{E}$, respectively.
Now by using (2.8), we have the following bounds:

$$\begin{cases} \left|\psi^{(k)}(x)\right|_{\bar{\Omega}} \leq C\left(1 + \varepsilon^{(2-k)}\right), & 0 \leq k \leq 3, \\ \left|\lambda^{(k)}(x)\right| \leq C\varepsilon^{-k}e^{-\alpha(1-x)/\varepsilon}, & 0 \leq k \leq 3, \quad \forall x \in \bar{\Omega}, \end{cases} \tag{3.18}$$

which becomes

$$\begin{cases} \mathcal{L}\psi(x) = \Phi(x), & \psi(0) = \lambda(0) = 0, \\ \mathcal{L}\lambda(x) = 0, & \psi(x_N) = -\lambda(1). \end{cases} \tag{3.19}$$

Therefore, we have shown that $\mathcal{L}^N(P^N - p)(x_i) = O(H^2) + \dfrac{1}{2}\mu(x_i)(x_{i+1} - x_i)p''(x)$ for all $x_i \in \Omega$.

The error in the smooth component P^N is determined in the following Lemma.

Lemma 3.4. *Under assumptions* $\varepsilon \leq N^{-1}$. *We have*

$$P^N(x_i) - p(x_i) = H\tilde{E}(x_i) + O(N^{-2}), \forall x_i \in [0, 1-\tau]$$

Proof Given $x_i \in (0,1)$ fixed, Taylor's expansion yields:

$$\left|(\mathcal{L} - \mathcal{L}^N)\right| \psi(x_i) \leq \left[\frac{\varepsilon}{3}(h_{i+1} + h_i)||\frac{\partial^3 \psi}{\partial x^3}|| + \frac{\mu(x_i)}{2}(h_{i+1} + h_i)||\frac{\partial^2 \psi}{\partial x^2}||\right].$$

Furthermore, using (3.18), we find:

$$\left|(\mathcal{L}^N - \mathcal{L})\psi(x_i)\right| \leq \frac{\varepsilon}{3}(h_{i+1} + h_i) + C\frac{\mu(x_i)}{2}(h_{i+1} + h_i) \leq C(h_{i+1} + h_i) + C(h_{i+1} + h_i) \leq CH.$$

From the truncation error, we have:

$$\mathcal{L}^N\psi(x_i) = \mathcal{L}\psi(x_i) + \mathcal{L}^N\psi(x_i) - \mathcal{L}\psi(x_i) = \mathcal{L}\psi(x_i) + O(H).$$

Thus, $H\mathcal{L}^N\psi(x_i) = H\Phi(x_i) + O(H^2)$. Considering that $h_i \leq H$, Lemma 3.3 yields

$$\mathcal{L}^N\left(P^N - p\right)(x_i) - H\mathcal{L}^N\psi(x_i) = \begin{cases} O(H^2) + \frac{1}{2}\mu(x_i)(h_{i+1} + h_i)p''(x_i) - H\Phi(x_i) - O(H^2), & x_i \in (0, 1-\tau), \\ (x_{i+1} - x_i - H)\Phi(x_i) + O(H^2), & x_i \in (1-\tau, 1), \end{cases} \tag{3.20}$$

$$\mathcal{L}^N\left(P^N - p - H\psi\right)(x_i) = O(H^2), \text{for} \quad x_i \in (0, 1-\tau], \tag{3.21}$$

$$\mathcal{L}^N\left(P^N - p - H\mathcal{L}^N\psi\right)(x_i) = O(H^2) + (h - H)\Phi(x_i), \text{for} \quad x_i \in (1-\tau, 1). \tag{3.22}$$

Now, let us define discrete mesh functions

$$M_i = C_3\left[N^{-2}(1 + x_i) + H\prod_{k=1}^{i}\left(1 + \frac{\alpha h_k}{2\varepsilon}\right)^{-1}\right] \quad \text{for} \quad i = 1, \ldots, N-1.$$

Then, apply the difference operators on M_i by using Lemma 3.2 and $\varepsilon \leq N^{-1}$ for $0 \leq i \leq N/2$, it follows that

$$\mathcal{L}^N M_i \geq C\frac{\prod_{k=1}^{i}\left(1 + \frac{\alpha h_k}{2\varepsilon}\right)}{\max\{\varepsilon, h_{i+1}\}}, \tag{3.23}$$

and for $N/2 < i \leq N$,

$$\mathcal{L}^N M_i \geq C_3 C_2 H\varepsilon^{-1}. \tag{3.24}$$

It is easy to check that $M_0 \geq 0 = \left|P^N(0) - p(0) - H\psi(0)\right|$ and $M_N \geq C_3 = \left|P^N(1) - p(1) - H\psi(1)\right|$. By choosing an adequately large value for C_3, it effectively operates as a barrier function denoted by M_i for $\pm\left[P^N(x_i) - p(x_i) - H\psi(x_i)\right]$. Employing the discrete maximum principle to the barrier function M_i, we subsequently ascertain:

$$M_i \geq P^N(x_i) - p(x_i) - H\psi(x_i), \quad x_i \in (0, 1-\tau).$$

Thus, for $i = 1, \ldots, N/2$, we have:

$$\left|P^N(x_i) - p(x_i - H\tilde{E}(x_i))\right| \leq \left|P^N(x_i) - p(x_i) - H\lambda(x_i)\right| + \left|H\psi(x_i)\right| \leq M_i + 2N^{-1}\left|\psi(x_i)\right| \leq CN^{-2}.$$

where we used $\tilde{E} = \psi + \lambda$.
Now we can show that extrapolation improves the accuracy of P^N on $(0, 1-\tau]$ interval.

Lemma 3.5. *For all $x_i \in [0, 1-\tau]$, we have achieved second-order convergence for the smooth component*

$$|p(x_i) - \left(P^{2N}(x_i) - P^N(x_i)\right)| \leq CN^{-2},$$

where C is a constant.
Proof. Let $x_i \in [0, 1-\tau]$. Since the subinterval mesh width of Ω_1^{2N} is half of those of Ω_1^N, and the function $\tilde{E}(.)$ depends on τ, we utilize Lemma 3.4 to deduce:

$$P^N - p(x_i) = H\tilde{E}(x_i) + O(N^{-2}).$$

Similarly, by maintaining a constant value for τ on the mesh Ω_1^{2N}, we obtain:

$$P^{2N} - p(x_i) = \frac{H}{2}\tilde{E}(x_i) + O(N^{-2}). \tag{3.25}$$

Using the extrapolation formulas (3.14), 3.4, and (3.25), we arrive to the following conclusion:

$$p(x_i) - \left(P^{2N}(x_i) - P^N(x_i)\right) = O(N^{-2}), \quad \text{for} \quad 1 \leq i \leq N/2.$$

The subsequent lemma demonstrates the error of $P^N(x_i)$ after extrapolating over $(1-\tau, 1]$.

Lemma 3.6. *Under assumptions $\varepsilon \leq N^{-1}$. For all $x_i \in [1-\tau, 1]$,*

$$\left|p(x_i) - \left(P^{2N}(x_i) - P^N(x_i)\right)\right| \leq C(N^{-1}(\ln N)^2).$$

for some constant C.
Proof. We define the function $\hat{G}(x)$ on $[1-\tau, 1]$ by

$$\mathcal{L}\hat{G}(x) = 0, \hat{G}(1-\tau(x_N)) = 1, \hat{G}(1) = 0, \quad \text{for} \quad (1-\tau, 1).$$

Within the domain Ω_1^N, we introduce a discrete approximation $\hat{G}^N$ of $\hat{G}$ as outlined below:

$$\mathcal{L}\hat{G}^N(x) = 0, \hat{G}(1-\tau(x_N)) = 1, \hat{G}^N(1) = 0, \quad \text{for} \quad N/2 \leq i \leq N.$$

For the convergence of the upwind scheme, we have

$$\left|\hat{G} - \hat{G}^N\right| \leq CN^{-1}\ln N \quad \text{for} \quad N/2 \leq i \leq N. \tag{3.26}$$

We define $\varphi(x) = P^N(x_i) - p(x_i) - \left(H\bar{E}(1-\tau)\right)\hat{G}(x_i) \quad \text{for} \quad N/2 \leq i \leq N.$
Then $\varphi(x_{N/2}) = O(N^{-2}), \varphi(x_N) = 0$ and

$$\mathcal{L}^N\varphi(x_i) = O(h_i) + O(H^2) = O(N^{-1}(\ln N)^2).$$

Using a barrier function of the form $C(1+x_i)N^{-1}(\ln N)^2$, we obtain the following estimate for $\varphi(x_i)$:

$$|\varphi(x_i)| \leq CN^{-1}(\ln N)^2, \quad \text{for} \quad N/2 \leq i \leq N. \tag{3.27}$$

Furthermore, noticing that $\left|\tilde{G}(1-\tau)\right| \leq C$, we can deduce the following relationship:

$$P^N(x_i) - p(x_i) = \left(H\tilde{G}(1-\tau)\right)\tilde{G}^N(x_i) + O(N^{-1}(\ln N)^2). \tag{3.28}$$

Similarly, on the mesh Ω^{2N}, one has

$$P^{2N} - p(x_i) = (\frac{H}{2})\tilde{E}(1-\tau)\tilde{G}(x_i) + O(N^{-1}(\ln N)^2), \quad \text{for} \quad N/2 \leq i \leq 2N. \tag{3.29}$$

Now combining (3.28) and (3.29), we obtain

$$p(x_i) - \left(2P^{2N} - P^N\right)(x_i) = 2(p - P^{2N})(x_i) - (p - P^N)(x_i) = O(N^{-1}(\ln N)^2), \quad \text{for} \quad N/2 \leq i \leq N.$$

3.3.3. Extrapolated solution of Q^N

The Richardson extrapolation is now utilized to approximate Q^N in Ω^N in the following lemmas. The error $Q^N(x_i) - q(x_i)$ is computed separately in the sub-intervals $[0, 1-\tau]$ and $[1-\tau, 1]$.

Lemma 3.7. *For all $x_i \in [0, 1-\tau]$, we have*

$$\left|q(x_i) - \left(2Q^{2N} - Q^N\right)(x_i)\right| \leq CN^{-2}.$$

Proof. Referring to (Theorem 1 of Cen [6]), we obtain:

$$\left|q_i - Q_i^N\right| \leq |q_i| + \left|Q_i^N\right| \leq Ce^{-\alpha x_i/\varepsilon} + CS_i'.$$

By employing Lemma 3.2, it is straightforward to establish that for $N/2 \leq i \leq N$,

$$\left|q_i - Q_i^N\right| \leq CN^{-2}.$$

To study the impact of extrapolation $(1-\tau, 1)$, we introduce the function F over the interval $[1-\tau, 1]$ through a BVP with IBC boundary conditions. Suppose F is the solution of the following BVPs with IBC:

$$\begin{cases} \mathcal{L}F(x_N) = \dfrac{2\varepsilon}{\alpha}\mu(x_i)q''(x), \quad x \in (1-\tau, 1), \\ F(1-\tau(x_N)) = F(1) = 0. \end{cases} \tag{3.30}$$

Then, F depends upon τ and independent of N. Now using the fact that $||F'(0)|| \leq C\varepsilon^{-1}$, we have for $0 \leq x \leq 1-\tau$

$$||F^{(k)}(x)|| \leq C\varepsilon^{-k}e^{-\alpha x/\varepsilon}, k = 1, 2, 3, 4. \tag{3.31}$$

Lemma 3.8. *For all $x_i \in [1-\tau, 1]$, we have*

$$Q^N(x_i) - q(x_i) = (N^{-1}\ln N)F(x_i) + O(N^{-2}(\ln N)^2). \tag{3.32}$$

Proof. The detailed proof is given [25, 36].
We will now illustrate how extrapolation improves the accuracy of $Q^N(x_i)$ for x_i within the range of $x_i \in [1-\tau, 1]$.

Lemma 3.9. *For some constant C and for all $x_i \in [1-\tau, 1]$, we have*

$$|q(x_i) - \left(2Q^{2N}(x_i) - Q^N(x_i)\right)| \leq CN^{-2}(\ln N)^2.$$

Proof. Assuming that $x_i \in [1-\tau, 1]$, we can reconfigure equation (3.32) to more explicitly showcase its reliance on the selection of both N and τ.

$$Q^N(x_i) - q(x_i) = N^{-1}\ln NF(x_i) + O(N^{-1}(\ln N)^2) = N^{-1}(\frac{\alpha\tau}{2\varepsilon})F(x_i) + O\left(N^{-1}(\frac{\alpha\tau}{2\varepsilon})^2\right) \tag{3.33}$$

Similarly,

$$Q^{2N}(x_i) - q(x_i) = N^{-1}(\frac{\alpha\tau}{2\varepsilon})F(x_i) + O\left(N^{-2}(\frac{\alpha\tau}{2\varepsilon})^2\right) \tag{3.34}$$

Given that $\bar{\Omega}_1^{2N}$ is solved utilizing the identical transition point $1-\tau$, it can be concluded that:

$$Q^{2N}(x_i) - q(x_i) = (2N)^{-2}(\frac{\alpha\tau}{2\varepsilon})F(x_i) + O\left(N^{-1}(\frac{\alpha\tau}{2\varepsilon})^2\right) \tag{3.35}$$

Replacing the first term (3.33) and (3.34), we have

$$q(x_i) - \left(2Q^{2N}(x_i) - Q^N(x_i)\right) \leq CN^{-2}(\ln N)^2$$

Hence, the desired result is required.

3.3.4. Convergence result of the solution Z^N

The main result of this paper is a theorem that proves a second-order error estimate, which is ε-uniform, for the solution obtained through Richardson extrapolation.

Theorem 3.10. *(Error after extrapolation) Assume that $\varepsilon \leq N^{-1}$, then there exists a positive constant C such that:*

$$\left|\xi(x_i) - \left(2Z^{2N}(x_i) - Z^N(x_i)\right)\right| \leq N^{-2}(\ln N)^2, \quad \textit{for} \quad x_i \in \Omega^N.$$

where C are positive constants.

Proof.

For each $x_i \in \Omega^N$, we have

$$\xi(x_i) - \left(2Z^{2N}(x_i) - Z^N(x_i)\right) = p(x_i) - \left(2P^{2N}(x_i) - P^N(x_i)\right) + q(x_i) - \left(2Q^{2N}(x_i) - Q^N(x_i)\right).$$

We obtain the desired result by combining the results of Lemmas 3.5, 3.6 for the smooth component and 3.7, 3.8, 3.9 for the layer component of the above equations.

4. Numerical Examples, Results and Discussion

We perform numerical tests to confirm theoretical findings, employing model problems from equations (2.1) and utilizing the numerical scheme in equation (3.5). This section presents two examples, and since exact solutions are unknown, we assess the maximum point-wise error using the double mesh principle [2, 25, 28]. To assess the accuracy of our approach, we compute the exact maximum pointwise absolute error provided by:

$$E^N_{\varepsilon,\text{exact}}(\varepsilon D^- Z) = \max_{0\leq i<N} \left|D^- Z(x_i) - \xi^-(x_i)\right|$$

For each N, we define ε-uniform maximum errors at the nodes as:

$$E^N_{\varepsilon,\text{exact}}(D^- Z) = \max_{\varepsilon} E^N_{\varepsilon,\text{exact}}(D^- Z_\varepsilon)$$

The calculation of the maximum pointwise double-mesh differences is given as follows:

$$E^N_\varepsilon(\varepsilon D^- Z) = \left|\left(D^- Z^N - D^- Z^{2N}\right)\right|.$$

where Z^N and Z^{2N} represent the numerical solutions acquired with N and $2N$ mesh intervals, respectively. We compute the ε-uniform maximum pointwise double-mesh differences, denoted as

$$E^N(\varepsilon D^- Z) = \max_{\varepsilon\in R_\varepsilon} E^N_\varepsilon.$$

In this case, R_N indicates the set of integer values examined for the number of mesh intervals. We define the computed corresponding ε-uniform numerical convergence rates for all N as:

$$S^N = \log 2\left(\frac{E^N}{E^{2N}}\right) \quad \text{and} \quad S^N_{\text{extp}} = \log 2\left(\frac{E^N_{\text{extp}}}{E^{2N}_{\text{extp}}}\right).$$

For each N in the range $R_N = 64, 128, 256, 512, 1024, 2048$ such that both N and $2N$ are in the set, we calculate ε-uniform maximum pointwise double-mesh differences $E^N(\varepsilon D^- Z)$. The numerical results are shown for ε values from $\varepsilon \in R_\varepsilon = \left\{2^{-20}, \ldots, 2^{-2}, 2^{-1}\right\}$, where R_ε define the ranges for the singular perturbation parameter.

Example 4.1. *Consider the following SPP:*

$$-\varepsilon\xi''(x) + (1+x)\xi'(x) = (1-x)^2, \quad x \in \Omega,$$

with boundary conditions

$$\xi(0) = 0, \quad \xi(1) - \varepsilon \int_0^1 \frac{x}{2}\xi(x)dx = 1.$$

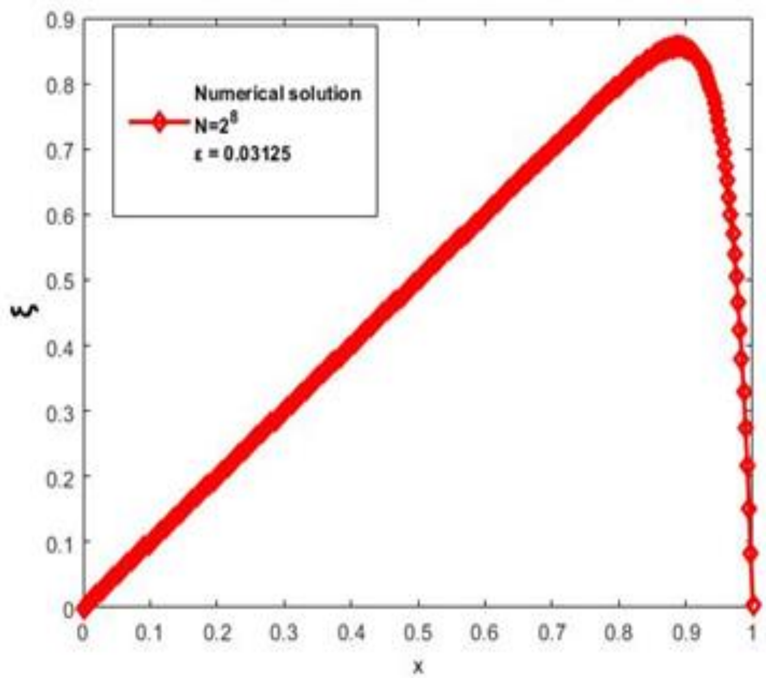

Figure 3: Graph of the numerical solution for $N = 256$ and $\varepsilon = 2^{-5}$ in Example 4.1.

Example 4.2. *Consider the following SPP:*

$$-\varepsilon\xi''(x) + \xi'(x) = 1, \quad x \in \Omega,$$

with boundary conditions

$$\xi(0) = 0, \quad \xi(1) - \varepsilon \int_0^1 \frac{x}{2}\xi(x)dx = 0.$$

Using the provided data, Tables 1 and 2 show calculated values of EN and SN for the scaled derivative of the solution εξ . Computation utilizes scaled discrete upwind method, shown in Examples 4.1 and 4.2. In Tables 3 and 4, we can find precise maximum pointwise errors and convergence rates for Examples 4.1 and 4.2. These tables indicate nearly first-order convergence. Additionally, the tables summarize the maximum pointwise errors and convergence orders for the examples. As we review the results in Tables 3 and 4, we will notice a consistent decrease in the computed ε-uniform errors EN for Examples 4.1 and 4.2 as N increases. This confirms the ε-uniform convergence of the upwind scheme (3.5) both before and after extrapolation.

We can see from the numerical solution plots in Figures 8 and ??, as well as the log-log plots of

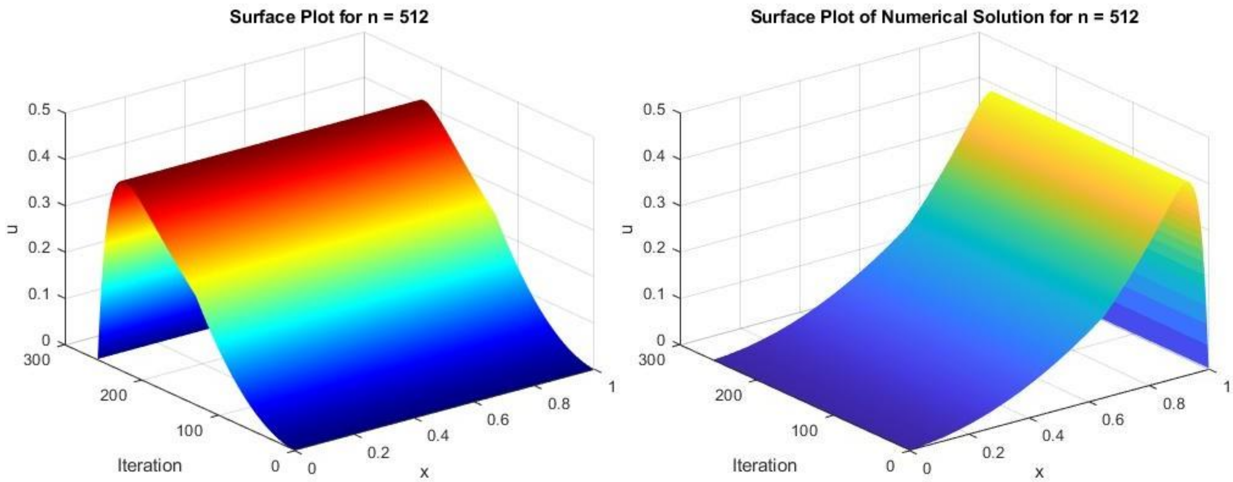

(a) for N = 512 and $\varepsilon = 2^{-5}$ using 4.1. (b) for N = 512 and $\varepsilon = 2^{-5}$ using 4.2.

Figure 4: Surface plot in Example 4.1 and 4.2

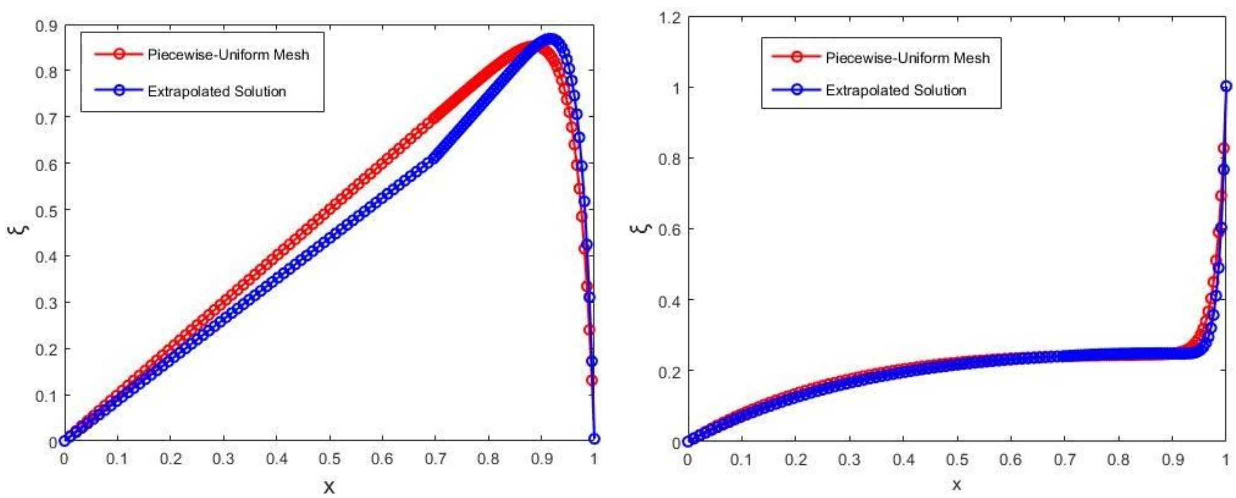

(a) for N = 256 and $\varepsilon = 2^{-5}$ using 4.1. (b) for N = 512 and $\varepsilon = 2^{-5}$ using 4.2.

Figure 5: Comparison of piecewise-uniform and extrapolated mesh in Example 4.1 and 4.2.

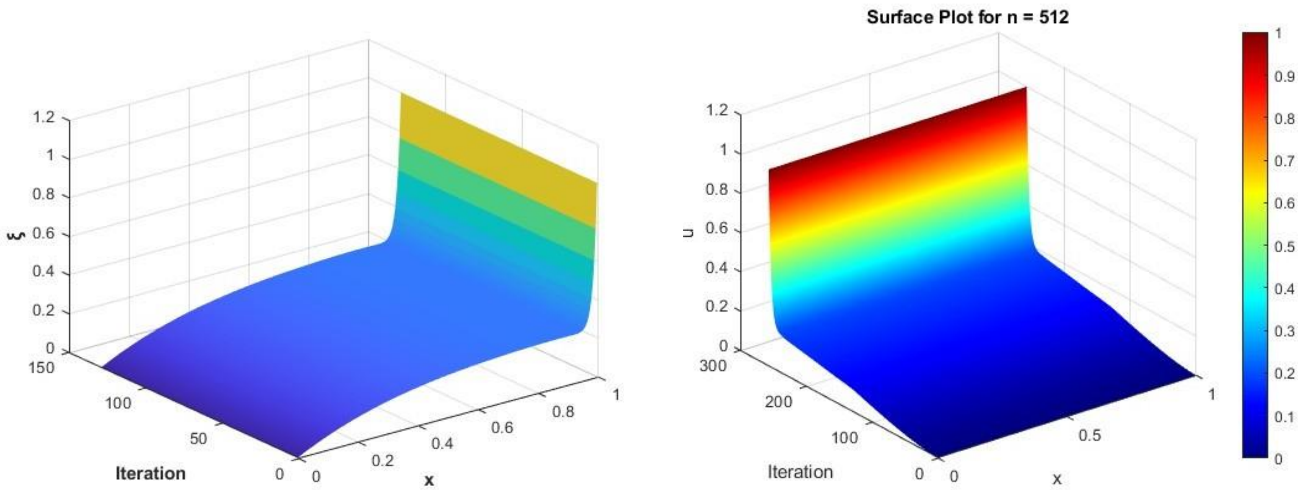

(a) for N = 512 and ε = 2−5 using 4.1. (b) for N = 512 and ε = 2−5 using 4.2.

Figure 6: Surface plot for exponential (eXp) mesh in Example 4.1 and 4.2.

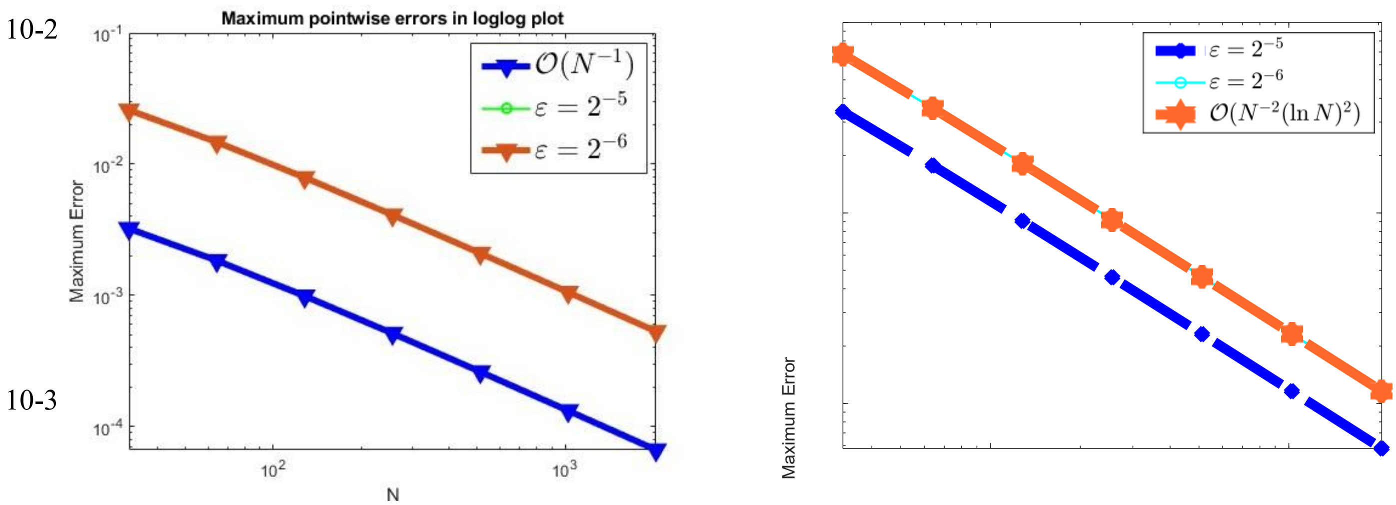

(a) Before Extrapolation. (b) After Extrapolation.

Figure 7: Log-log plot of maximum errors in Example 4.1.

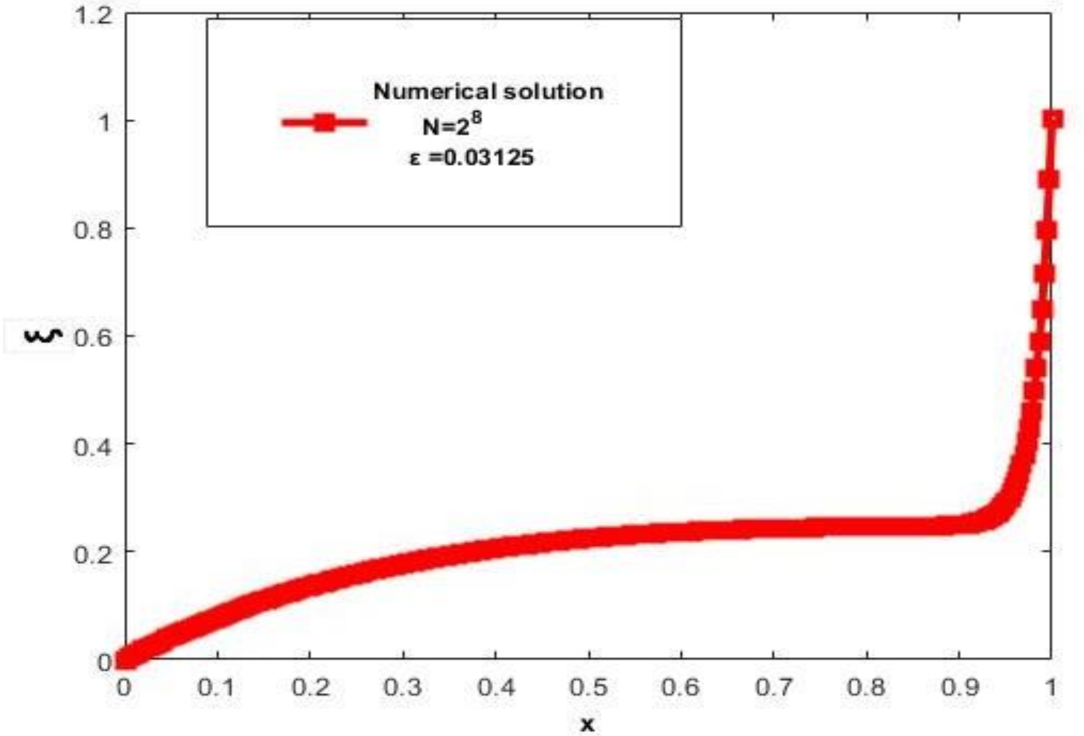

Figure 8: Graph of the numerical solution for N = 256 and ε = 2−5 in Example

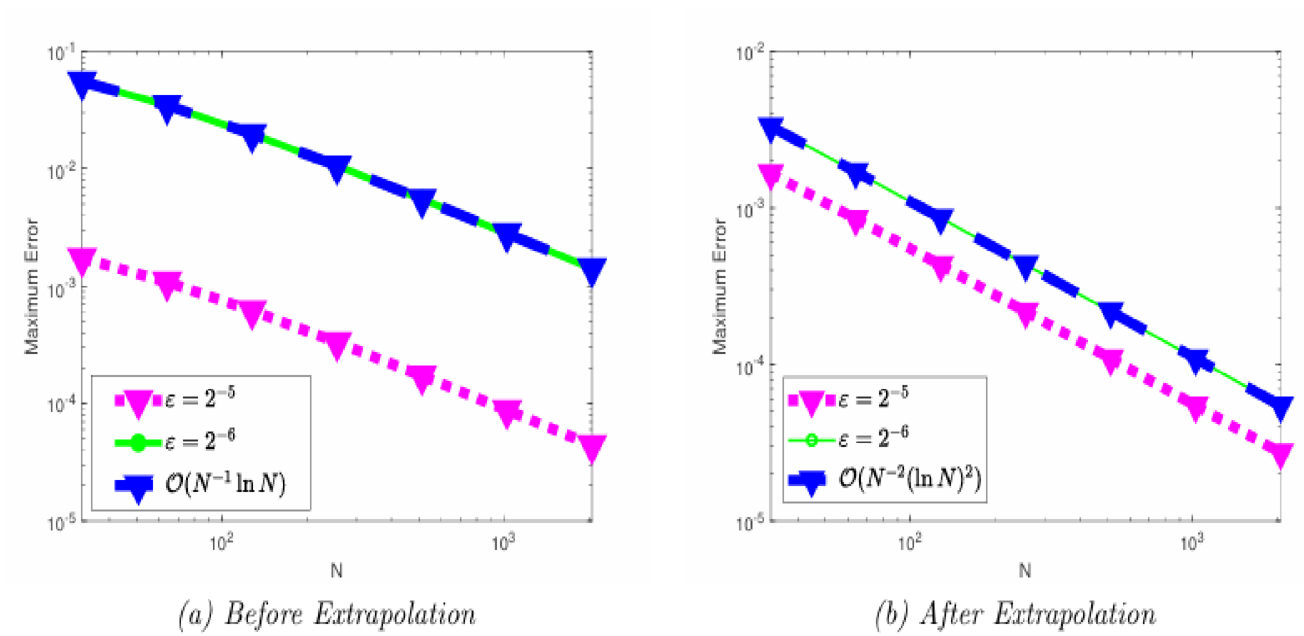

Figure 9: The log-log plot of the maximum pointwise errors using exponential (eXp) mesh for Example 4.2.

Table 1: Values of E^N and S^N for the solution of ξ for Example 4.1.

$\varepsilon \backslash N$	64	128	256	512	1024	2048
2^{-1}	3.5500e-03	1.8160e-03	9.1857e-04	4.6197e-04	2.3166e-04	1.1600e-04
2^{-3}	1.4720e-02	7.9031e-03	4.1015e-03	2.0902e-03	1.0553e-03	5.3022e-04
2^{-6}	2.3427e-02	1.5490e-02	9.7590e-03	5.8112e-03	3.3469e-03	1.8832e-03
2^{-9}	2.0704e-02	1.2767e-02	7.5627e-03	4.3494e-03	2.4481e-03	1.3565e-03
2^{-12}	2.0707e-02	1.2768e-02	7.5643e-03	4.3506e-03	2.4488e-03	1.3569e-03
2^{-15}	2.0706e-02	1.2768e-02	7.5642e-03	4.3506e-03	2.4488e-03	1.3570e-03
2^{-20}	2.0706e-02	1.2768e-02	7.5642e-03	4.3506e-03	2.4488e-03	1.3570e-03
E^N (Solution ξ)	**2.3427e-02**	**1.5490e-02**	**9.7590e-03**	**5.8112e-03**	**3.3469e-03**	**1.8832e-03**
S^N (Solution ξ)	**0.5968**	**0.6665**	**0.7479**	**0.7960**	**0.8296**	**-**
2^{-1}	1.7750e-03	9.0801e-04	4.5929e-04	2.3098e-04	1.1583e-04	5.8000e-05
2^{-3}	1.8400e-03	9.8788e-04	5.1268e-04	2.6128e-04	1.3191e-04	6.6277e-05
2^{-6}	3.2208e-04	1.9888e-04	1.1788e-04	6.7813e-05	3.8171e-05	2.1152e-05
2^{-9}	4.3649e-05	2.4935e-05	1.4771e-05	8.4950e-06	4.7813e-06	2.6495e-06
2^{-12}	5.0554e-06	3.1173e-06	1.8468e-06	1.0622e-06	5.9784e-07	3.3128e-07
2^{-15}	6.3191e-07	3.8965e-07	2.3084e-07	1.3277e-07	7.4731e-08	4.1411e-08
2^{-17}	1.5798e-07	9.7412e-08	5.7710e-08	3.3193e-08	1.8683e-08	1.0353e-08
2^{-20}	2.1161e-08	1.4085e-08	8.8689e-09	5.2990e-09	3.0561e-09	1.7213e-09
E^N (Solution ξ)	**1.8400e-03**	**9.8788e-04**	**5.1268e-04**	**2.6128e-04**	**1.3191e-04**	**6.6277e-05**
S^N (Solution ξ)	**0.8973**	**0.9463**	**0.9725**	**0.9860**	**0.9930**	**-**

Table 2: Values of E^N and S^N for the solution of ξ for Example 4.2.

$\varepsilon \backslash N$	64	128	256	512	1024	2048
2^{-1}	1.7018e-03	8.6234e-04	4.3406e-04	2.1776e-04	1.0906e-04	5.4576e-05
2^{-3}	1.0520e-02	5.4609e-03	2.7833e-03	1.4052e-03	7.0603e-04	3.5388e-04
2^{-6}	4.8788e-03	2.4950e-03	1.2620e-03	6.3466e-04	3.1825e-04	1.5936e-04
2^{-9}	2.0704e-02	1.2767e-02	7.5627e-03	4.3494e-03	2.4481e-03	1.3565e-03
2^{-12}	2.0707e-02	1.2768e-02	7.5643e-03	4.3506e-03	2.4488e-03	1.3569e-03
2^{-15}	2.0706e-02	1.2768e-02	7.5642e-03	4.3506e-03	2.4488e-03	1.3570e-03
2^{-17}	2.0706e-02	1.2768e-02	7.5642e-03	4.3506e-03	2.4488e-03	1.3570e-03
2^{-20}	2.0706e-02	1.2768e-02	7.5642e-03	4.3506e-03	2.4488e-03	1.3570e-03
E^N (Solution ξ)	**2.0706e-02**	**1.2768e-02**	**7.5642e-03**	**4.3506e-03**	**2.4488e-03**	**1.3570e-03**
S^N (Solution ξ)	**0.6975**	**0.7553**	**0.7980**	**0.8291**	**0.8517**	**-**
2^{-1}	8.5088e-04	4.3117e-04	2.1703e-04	1.0888e-04	5.4531e-05	2.7288e-05
2^{-3}	1.3151e-03	6.8261e-04	3.4791e-04	1.7565e-04	8.8254e-05	4.4235e-05
2^{-6}	3.2208e-04	1.9888e-04	1.1788e-04	6.7813e-05	3.8171e-05	2.1152e-05
2^{-9}	4.0438e-05	2.4935e-05	1.4771e-05	8.4950e-06	4.7813e-06	2.6495e-06
2^{-12}	5.0554e-06	3.1173e-06	1.8468e-06	1.0622e-06	5.9784e-07	3.3128e-07
2^{-15}	6.3191e-07	3.8965e-07	2.3084e-07	1.3277e-07	7.4731e-08	4.1411e-08
2^{-17}	1.5798e-07	9.7412e-08	5.7710e-08	3.3193e-08	1.8683e-08	1.0353e-08
2^{-20}	1.9747e-08	1.2177e-08	7.2138e-09	4.1491e-09	2.3354e-09	1.2941e-09
E^N (Solution ξ)	**1.3151e-03**	**6.8261e-04**	**3.4791e-04**	**1.7565e-04**	**8.8254e-05**	**4.4235e-05**
S^N (Solution ξ)	**0.9460**	**0.9723**	**0.9860**	**0.9930**	**0.9965**	**-**

maximum pointwise errors in Figures 7 and 10, that Richardson extrapolation effectively increases the order of convergence of the upwind scheme. The upwind scheme's order of convergence improves from O N^{-1} ln N to O N^{-2} $\ln^2$ N , which is consistent with the theoretical bounds established in Theorems 3.1 and 3.10. These experimental results validate the effectiveness of Richardson extrapolation.

CONCLUSION

We used the Richardson extrapolation applied to an upwind finite difference method on Shishkin mesh and exponential (eXp) mesh to solve singularly perturbed second-order convection-diffusion problems (2.1) with integral boundary conditions. The behavior of the continuous solution of the problem is investigated and proven to satisfy the continuous stability estimate. The integral boundary condition is addressed using numerical integration techniques, namely the trapezoidal rule.

We discretized the domain using a piecewise-uniform mesh and exponential (eXp) by utilized the upwind finite difference scheme. To handle the integral boundary conditions, we employed the trapezoidal rule for numerical integration. The findings from these articles indicate a robust application of Richardson extrapolation techniques across various types of singularly perturbed convection-diffusion problems, including those with integral and non-local boundary conditions. The use of Shishkin and other graded meshes is prevalent, showcasing their effectiveness in enhanc- ing numerical accuracy. The novel approach described in the query aligns well with these studies, particularly in its focus on integral boundary conditions and the combination of different mesh types.

Table 3: Maximum point-wise errors and the corresponding order of convergence using before and after extrapolation for Example 4.1.

$\varepsilon \downarrow$	Extrapolation	Number of Mesh Intervals N					
		64	128	256	512	1024	2048
2^{-1}	Before	1.7750e-03	9.0801e-04	4.5929e-04	2.3098e-04	1.1583e-04	5.8000e-05
		0.9356	0.96705	9.8332	0.9916	0.9978	
	After	5.5469e-05	1.4188e-05	3.5882e-06	9.0228e-07	2.2623e-07	5.664e-08
		1.9357	1.967	1.9833	1.9916	1.9958	
2^{-2}	Before	2.0200e-03	1.0499e-03	5.3540e-04	2.7039e-04	1.3588e-04	6.8110e-05
		0.8928	0.9441	0.9714	0.9855	0.9927	
	After	1.2625e-4	3.2808e-05	8.3656e-06	2.1124e-06	5.3077e-07	1.3303e-07
		1.8928	1.9442	1.9715	1.9856	1.9927	
2^{-3}	Before	1.8400e-03	9.8788e-04	5.1268e-04	2.6128e-04	1.3191e-04	6.6277e-05
		0.8110	0.8973	0.9462	0.9724	0.9860	
	After	2.3001e-4	6.1743e-05	1.6021e-05	4.0824e-06	1.0305e-06	2.589e-07
		1.811	1.8973	1.9463	1.9725	1.9861	
2^{-4}	Before	1.5855e-03	9.0435e-04	4.8573e-04	2.5213e-04	1.2851e-04	6.4882e-05
		0.4702	0. 8099	0.8967	0.9459	0.9723	
	After	3.9637e-04	1.1304e-04	3.0358e-05	7.8791e-06	2.0079e-06	5.0689e-07
		1.811	1.8973	1.9463	1.9725	1.9861	
2^{-5}	Before	7.6736e-04	5.0594e-04	3.1774e-04	1.8858e-04	1.0843e-04	6.0910e-05
		0.4087	0.6009	0. 6711	0.7526	0.7983	
	After	3.8368e-4	1.2649e-4	3.9717e-05	1.1786e-05	3.3884e-06	9.5172e-07
		1.4087	1.6009	1.6711	1.7527	1.7984	
2^{-6}	Before	3.2208e-04	1.9888e-04	1.1788e-04	6.7813e-05	3.8171e-05	2.1152e-05
		0.4028	0.5687	0.6716	0.8106	0.8971	
	After	3.5656e-4	1.1825e-4	3.7243e-05	1.1106e-05	3.2004e-06	9.0079e-07
		1.4085	1.5922	1.6669	1.7456	1.7951	
E^N	Before	**2.0200e-03**	**1.0499e-03**	**5.3540e-04**	**2.7039e-04**	**1.3588e-04**	**6.8110e-05**
S^N		**0.9441**	**0.9716**	**0.9856**	**0.9927**	**0.9964**	
E^N_{extp}	After	**3.8368e-4**	**1.2649e-4**	**3.9717e-05**	**1.1786e-05**	**3.3884e-06**	**9.5172e-07**
S^N_{extp}		**1.6009**	**1.6712**	**1.7527**	**1.7984**	**1.8320**	

In addition, we utilized the Richardson extrapolation method to greatly enhance accuracy, resulting in nearly a second-order convergence rate. Our analysis revealed an improvement in convergence rate from about O ($N^{-1}\ln N$) to O ($N^{-2}\ln^2 N$) with respect to ε, leading to more dependable and precise solutions with fewer errors at the nodes. We presented two instances that illustrated the highest pointwise errors and convergence rates for different values of ε and N . The convergence rate improves approximately from first-order O (N^{-1}) to nearly second-order O ($N^{-2}(\ln N)^2$ concerning ε, as seen in the order of convergence: The overall result of our investigation suggests that using extrapolation decreases nodal errors and increases the numerical method's convergence rate. The experimental results align with the theoretical bounds established in Theorems 3.10 and ??. Two examples validate the effectiveness of the numerical method, displaying maximum pointwise errors and convergence rates for different ε and N. Finally, a comparison is made that demonstrates how post-processing techniques produce better, more accurate results. Future work could extend this method to handle problems with two parameters, PDE, and equations with a discontinuous source term with non-local boundary conditions. The above method can be extended to problems.

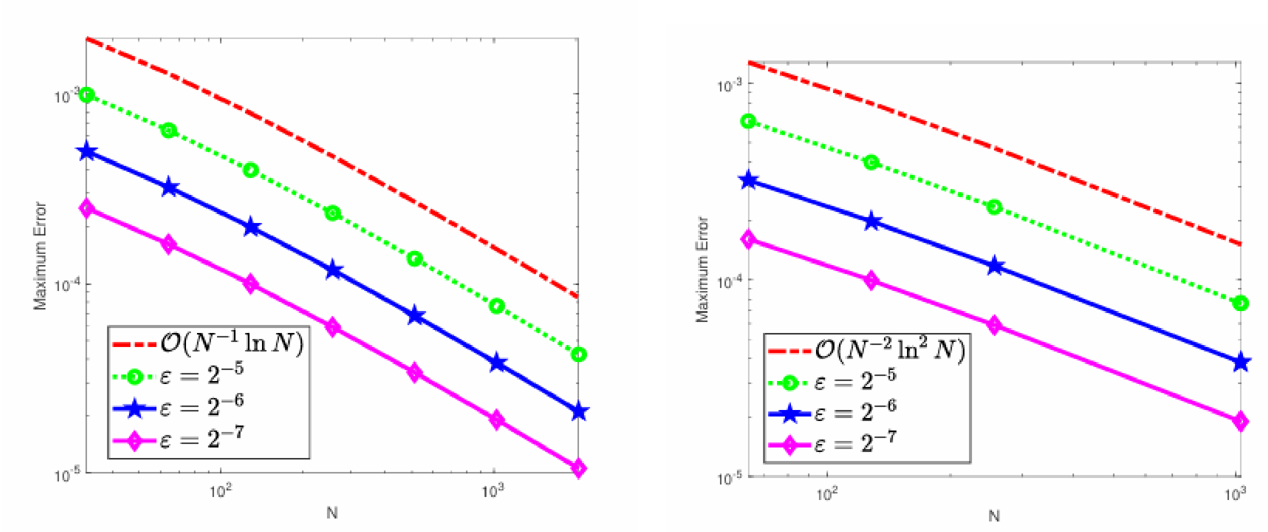

(a) Before Extrapolation *(b) After Extrapolation*

Figure 10: The log-log plot of the maximum pointwise errors using Shishkin mesh for Example 4.2.

With two parameter, partial differential equations and also equations with discontinuous source term with integral boundary conditions.

Table 4: Maximum point-wise errors and the corresponding order of convergence using before and after extrapolation for Example 4.2.

$\varepsilon \downarrow$	Extrapolation	Number of Mesh Intervals N					
		64	128	256	512	1024	2048
2^{-1}	Before	8.5088e-04	4.3117e-04	2.1703e-04	1.0888e-04	5.4531e-05	2.7288e-05
		0.9623	0.9807	0.9903	0.9951	0.9975	
	After	2.659e-05	6.737e-06	1.6955e-06	4.2531e-07	1.0651e-07	2.6649e-08
		1.9623	1.9807	1.9904	1.9952	1.9976	
2^{-2}	Before	1.2197e-03	6.2376e-04	3.1550e-04	1.5866e-04	7.9562e-05	3.9839e-05
		0.9339	0.9674	0.9833	0.9916	0.9958	
	After	7.6231e-05	4.9296e-06	1.2396e-06	3.1079e-07	7.7810e-08	7.9644e-08
		1.9340	1.9675	1.9834	1.9916	1.9958	
2^{-3}	Before	1.3151e-03	6.8261e-04	3.4791e-04	1.7565e-04	8.8254e-05	4.4235e-05
		0.8965	0.9459	0.9723	0.9860	0.9929	
	After	1.6438e-4	4.2663e-05	1.0872e-05	2.7445e-06	6.8948e-07	1.7279e-07
		1.8966	1.946	1.9724	1.986	1.9929	
2^{-4}	Before	1.2331e-03	6.6178e-04	3.4338e-04	1.7498e-04	8.8334e-05	4.4381e-05
		0.8122	0.8978	0.9465	0.9726	0.9861	
	After	3.2354e-4	9.9752e-05	2.9547e-05	8.4965e-06	2.3911e-06	6.6248e-07
		1.6308	1.6975	1.7554	1.798	1.8292	
2^{-5}	Before	6.4174e-04	3.9682e-04	2.3530e-04	1.3537e-04	7.6197e-05	4.2223e-05
		0.6735	0.8116	0.8975	0.9464	0.9725	
	After	3.2087e-4	9.9206e-05	2.9412e-05	8.4603e-06	2.3811e-06	6.5974e-07
		1.6173	1.6935	1.754	1.7976	1.8291	
2^{-6}	Before	8.6615e-04	5.4320e-04	3.0952e-04	1.6616e-04	8.6226e-05	4.3942e-05
		0.5849	0.6731	0.8114	0.8975	0.9463	
	After	3.2354e-4	9.9751e-05	2.9548e-05	8.4973e-06	2.3914e-06	6.6258e-07
		1.6250	1.6955	1.7545	1.7977	1.8291	
E^N	Before	**1.3151e-03**	**6.8261e-04**	**3.4791e-04**	**1.7565e-04**	**8.8254e-05**	**4.4235e-05**
S^N		**0.9460**	**0.9723**	**0.9860**	**0.9930**	**0.9965**	
E^N_{extp}	After	**3.2354e-4**	**9.9752e-05**	**2.9548e-05**	**8.4973e-06**	**2.3914e-06**	**6.6258e-07**
S^N_{extp}		**1.6975**	**1.7553**	**1.7980**	**1.8291**	**1.8517**	

REFERENCES

[1] G. AMIRALIYEV, I. AMIRALIYEVA, AND M. KUDU, A numerical treatment for singularly perturbed differential equations with integral boundary condition, Applied mathematics and computation, 185 (2007), pp. 574—582.

[2] G. AMIRALIYEV AND M. CAKIR, Numerical solution of the singularly perturbed problem with nonlocal boundary condition, Applied Mathematics and Mechanics, 23 (2002), pp. 755—764.

[3] D. BOFFI, Convection-diffusion problems. an introduction to their analysis and numerical solution., 2020.

[4] M. CAKIR AND G. M. AMIRALIYEV, A finite difference method for the singularly perturbed problem with nonlocal boundary condition, Applied mathematics and computation, 160 (2005), pp. 539-549.

[5] A second order numerical method for singularly perturbed problem with non-local boundary condition, Journal of Applied Mathematics and Computing, 67 (2021), pp. 919—936.

[6] Z. CEN, Parameter-uniform finite difference scheme for a system of coupled singularly perturbed convection—diffusion equations, International Journal of Computer Mathematics, 82 (2005), pp. 177-192.

[7] R. CIEGIS, The numerical solution of singularly perturbed nonlocal problem, Lietuvas Maternatica Rink, 28 (1988), pp. 144—152.

[8] C. CLAVERO, J. L. GRACIAt AND F. LISBONA, High order methods on shishkin meshes for singular perturbation problems of convection—diffusion type, Numerical Algorithms, 22 (1999), PP. 73-97.

[9] P. CONSTANTINOU AND C. XENOPHONTOS, Finite element analysis of an exponentially graded mesh for singularly perturbed problems, Computational Methods in Applied Mathematics, 15 (2015), pp. 135-143.

[10] H. G. DEBELA AND G. F. DURESSA, Accelemted exponentially fitted operator method for singularly perturbed problems with integrul boundary condition, International Journal of Differential Equations, 2020 (2020), pp. 1—8.

[11] Uniformly convergent numerical method for singularly perturbed convection-diffusion type problems with nonlocal boundary condition, International Journal for Numerical Methods in Fluids, 92 (2020), pp. 1914-1926.

[12] H. G. DEBELA, M. M. WOLDAREGAY, AND G. F. DURESSA, Robust numerical method for singularly perturbed convection-diffusion type problems with non-local boundary condition, Mathematical Modelling and Analysis, 27 (2022), pp. 199—214.

[13] P. FARRELL, A. HEGARTY, J. M. MILLER, E. O'RIORDAN, AND G. I. SHISHKIN, Robust computational techniques for boundary layers, CRC Press, 2000.

[14] J. GRACIA AND C. CLAVERO, Richardson extmpolation on generalized shishkin meshes for singularly perturbed problems, Monografias del Seminario Matemåtico Garcia de Galdeano, 31 (2004), pp. 169-178.

[15] M. K. KADALBAJOO AND V. GUPTA, A brief survey on numerical methods for solving singularly perturbe problems, Applied mathematics and computation, 217 (2010), pp. 3641—3716.

[16] H. B. KELLER, Numerical methods for two-point boundary-value problems, Courier Dover Publications, 2018.

[17] N. KOPTEVA AND N'l. STYNES, Approximation of derivatives in a convection—diffusion two-point boundary value problem, Applied numerical mathematics, 39 (2001), pp. 47—60.

[18] M. KUDU AND G. N"l. AMIRALIYEV, Finite difference method for a singularly perturbed differential equations with integml boundary condition, Int. J. Math. Comput, 26 (2015), pp. 71—79.

[19] T. LINSS, An upwind difference scheme on a novel shishkin-type mesh for a linear convection diffusion problem, Journal of computational and applied mathematics, 110 (1999), pp. 93—104.

[20] T. LINSS, Error expansion for a first-order upwind difference scheme, in PAMM: Proceedings in Applied Mathematics and Mechanics, vol. 2, Wiley Online Library, 2003, pp. 487—488.

[21] N. Mbroh, R. Guiem, and S. Noutchie, A second order numerical scheme for a singu larly perturbed convection diffusion problem with a non-local boundary condition., Journal of Analysis & Applications, 20 (2022).

[22] J. J. Miller, E. O'riordan, and G. I. Shishkin, Fitted numerical methods for singular perturbation problems: error estimates in the maximum norm for linear problems in one and two dimensions, World scientific, 1996.

[23] J. B. Munyakazi and K. C. Patidar, On richardson extrapolation for fitted operator finite difference methods, Applied Mathematics and Computation, 201 (2008), pp. 465–480.

[24] R. Mythili Priyadharshini and N. Ramanujam, Approximation of derivative for a singu larly perturbed second-order ordinary differential equation of robin type with discontinuous con vection coefficient and source term, Numer. Math. Theory Methods Appl.(to appear), (2009).

[25] M. C. Natividad and M. Stynes, Richardson extrapolation for a convection–diffusion prob lem using a shishkin mesh, Applied Numerical Mathematics, 45 (2003), pp. 315–329.

[26] P. C. Podila and V. Sundrani, A non-uniform haar wavelet method for a singularly per turbed convection–diffusion type problem with integral boundary condition on an exponentially graded mesh, Computational and Applied Mathematics, 42 (2023), p. 216.

[27] R. M. Priyadharshini and N. Ramanujam, Approximation of derivative to a singularly perturbed second-order ordinary differential equation with discontinuous convection coefficient using hybrid difference scheme, International Journal of Computer Mathematics, 86 (2009), pp. 1355–1365.

[28] V. Raja and A. Tamilselvan, Fitted finite difference method for third order singularly perturbed convection diffusion equations with integral boundary condition, Arab Journal of Mathematical Sciences, 25 (2019), pp. 231–242.

[29] A difference scheme on shishkin mesh for convection diffusion problems with integral boundary condition, in AIP Conference Proceedings, vol. 2277, AIP Publishing LLC, 2020, p. 190001.

[30] H.-G. Roos, M. Stynes, and L. Tobiska, Robust numerical methods for singularly per turbed differential equations: convection-diffusion-reaction and flow problems, vol. 24, Springer Science & Business Media, 2008.

[31] A. Samarskii, The theory of difference schemes, vol. 240, CRC Press, 2001.

[32] D. S. Sheiso and S. A. Kuchibhotla, Comparison of the coupled solution of the species, mass, momentum, and energy conservation equations by unstructured fvm, fdm, and fem.

[33] D. Sodano, Richardson extrapolation technique for singularly perturbed convection-diffusion problem with non-local boundary conditions, Available at SSRN 4774937, (2024).

[34] Richardson extrapolation technique for singularly perturbed parabolic convection-diffusion problems with a discontinuous initial condition, Asian Journal of Pure and Applied Mathemat ics, 6(1), 1–25, (2024).

[35] An upwind finite difference method to singularly perturbed parabolic convection-diffusion problems with discontinuous initial conditions on a piecewise-uniform mesh, Mendeley Data, V2 (2024).

[36] M. Stynes and L. Tobiska, A finite difference analysis of a streamline diffusion method on a shishkin mesh, Numerical Algorithms, 18 (1998), pp. 337–360.

[37] C. Xenophontos, S. Franz, and L. Ludwig, Finite element approximation of convection diffusion problems using an exponentially graded mesh, Computers & Mathematics with Ap plications, 72 (2016), pp. 1532–1540.